

$\hbar = 0$ . The upper curve is for a bulk spin wave in an infinite antiferromagnet with a propagation vector having a vanishing component normal to the surface. Examination of the eigenvectors of these states shows that the amplitude of the spin excitation decreases in a complicated exponential manner with increasing depth into the crystal.<sup>6</sup> In general, the rate of decrease of excitation amplitude increases with increasing  $E$  for fixed  $\epsilon_{\parallel}$  and also increases for decreasing  $\epsilon_{\parallel}$  at fixed  $E$ . The surface modes have excitation energies lower than that of the corresponding bulk states and consequently lead to a more rapid decrease in the surface magnetization. The surface modes are also characterized by very flat dispersion curves. This feature suggests that over much of  $k$  space the surface-spin-wave band could be approximated by a single excitation level and it is just this circumstance that is required for the validity of a molecular-field model.

It is interesting to note that surface waves exist for the antiferromagnet with nearest-neighbor coupling even for the case in which there is no perturbation in the surface exchange or surface anisotropy field, while in the case of the ferromagnet such perturbations are necessary in order to produce surface states.<sup>7</sup>

At finite temperatures additional terms enter

the equations for the surface states so that the surface-spin-wave dispersion curves depend upon temperature in manner more complicated than the usual thermal energy renormalization.

<sup>1</sup>P. W. Palmberg, R. E. De Wames, and L. A. Vredevoe, *Phys. Rev. Letters* **21**, 682 (1968).

<sup>2</sup>P. W. Palmberg, R. E. De Wames, L. A. Vredevoe, and T. Wolfram, to be published.

<sup>3</sup>E. G. MacRae, *J. Chem. Phys.* **45**, 3258 (1966).

<sup>4</sup>W. L. Roth, *Phys. Rev.* **111**, 772 (1958).

<sup>5</sup>The spectrum for antiferromagnetic surface spin waves on the [100] surface of a bcc crystal (which has spins of only one sublattice on the surface) has been derived by Mills and Saslow for the case in which the surface exchange is unperturbed; see D. L. Mills and W. M. Saslow, *Phys. Rev.* **171**, 448 (1968). Since exchange scattering from antiferromagnetics can be observed only from surfaces containing spins of both sublattices and since the effect of the reduced surface exchange is of central importance here, it is necessary to develop more general expressions.

<sup>6</sup>In the case of a surface containing spins of both sublattices the surface-state eigenvectors are quite complex. The amplitude of excitation depends upon two functions which decrease exponentially with distance from the surface as well as a sublattice structure factor.

<sup>7</sup>B. N. Filippov, *Fiz. Tverd. Tela* **9**, 1339 (1967) [translation: *Soviet Phys.-Solid State* **9**, 1048 (1967)].

## EFFECT OF NUCLEAR DEFORMATION ON FAST-NEUTRON TOTAL CROSS SECTIONS\*

Dale W. Glasgow and D. Graham Foster, Jr.

Battelle Memorial Institute, Pacific Northwest Laboratory, Richland, Washington

(Received 25 November 1968)

We have observed the effect of nuclear deformation on the fast-neutron total cross sections of 15 deformed nuclei within the region  $152 \leq A \leq 189$ , and five deformed nuclei within the region  $228 \leq A \leq 240$ . The phenomenological nonlocal optical model of Perey and Buck disagrees in these regions with our experimental data.

We have finished a large-scale program<sup>1</sup> of measurements of fast-neutron total cross sections for 78 naturally occurring elements and 14 separated isotopes. The measurements included all of the elements from H to Pu with the exception of the six inert gases and the highly radioactive elements near radium. The cross sections were measured with a pulsed-beam time-of-flight system at about 240 different energies per element to a statistical precision varying from

2.0 to 0.6% for  $3.0 \leq E_n \leq 15.0$  MeV and an energy resolution of 2.5 to 4.5% over the same limits. Previous measurements were essentially nonexistent over this energy range for the heavier alkali metals and alkaline earths, rare and expensive metals, the rare earths, various actinides, and most of the 14 separated isotopes. A detailed analysis of the data will be published shortly.

We emphasize the point that the large range in

energy and mass number of the  $\sigma_T$  data imposes rigid constraints upon any theoretical analysis. Furthermore, the existence of systematic trends and deviations should be revealed, since this large block of homogeneous data has been subjected uniformly to any unknown systematic errors. In addition, these are the only existing  $\sigma_T$  data over this energy range for 37 of the elements, 24 of which consist of spherical nuclei and 13 of which consist of highly deformed nuclei.

We have assumed in this Letter that the phenomenological, spherical, nonlocal optical potential of Perey and Buck<sup>2</sup> provides the correct energy variation of the neutron total cross sections for all spherical nuclei, and that any gross deviations of the theory from the data may be correlated with nuclear deformation. Specifically we searched for deviations in the regions  $Z > 50, N < 82, 152 \leq A \leq 186$ , and  $228 \leq A \leq 240$ . Many of the energy levels of nuclei in these regions correspond to states formed by collective vibrations and rotations of the nucleus. Since these states may be considered to be deformed, their associated optical potentials will also exhibit a deformed nature.

The neutron total cross section was calculated at 14 energies spanning the energy range 3.0-15.0 MeV for all the measured elements and separated isotopes above <sup>44</sup>Ca. The optical parameters are those of Ref. 2, namely  $V = 71$  MeV,  $W_d = 15$  MeV,  $V_{SO} = 7.2$  MeV,  $r_0 = 1.22$  F,  $a_s = 0.65$  F,  $a_d = 0.47$  F, and  $\beta = 0.85$  F.

The theoretical and experimental results agree to within 3% over the energy range 3.0-15.0 MeV for the spherical nuclei of <sup>45</sup>Sc, Ti, <sup>51</sup>V, Cr, <sup>53</sup>Cr, <sup>55</sup>Mn, Fe, <sup>59</sup>Co, Ni, Cu, Zn, Ga, Ge, <sup>75</sup>As, Se, Br, Rb, Sr, <sup>89</sup>Y, Zr, <sup>93</sup>Nb, Mo, <sup>99</sup>Tc, Ru, <sup>103</sup>Rh, Pd, Ag, Cd, <sup>115</sup>In, and Sn. Furthermore, the disagreement is  $\leq 1\%$  over 70% of the energy range of these 30 elements and separated isotopes. Figure 1 shows the comparison of three typical cases, <sup>53</sup>Cr, <sup>93</sup>Nb, and <sup>115</sup>In, with the theoretical predictions. The curves are the theoretical results while the points are sliding seven-channel averages (2 resolution widths) of the experimental cross sections. The standard deviations of the averaged total cross sections for the lighter nuclei at the higher energies are less than the size of the points. The excellent agreement between the data and the theoretical results supports the previous assumption that the nonlocal optical potential of Perey and Buck adequately describes the energy variation of  $\sigma_T$  for spherical nuclei as expected.

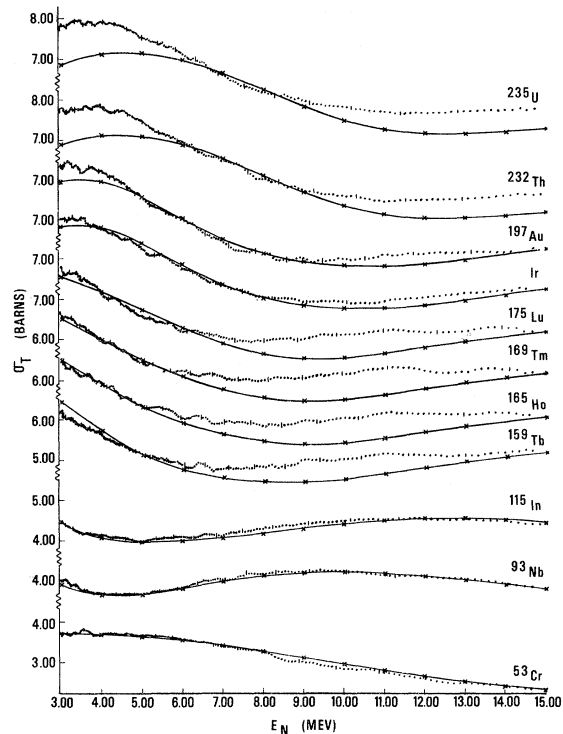


FIG. 1. Experimental and calculated neutron total cross sections versus neutron energy for selected spherical and deformed nuclei.

The total cross section for the interaction of a neutron with a deformed nucleus consists of contributions due to elastic scattering from the deformed ground state, inelastic excitation of the collective states, and all other reactions. Since the two scattering processes typically provide the major contributions to the neutron total cross section, quantitative effects of nuclear deformation should easily be observed in high-precision ( $\approx 1.0\%$ ) total cross-section data.

It has been postulated<sup>3,4</sup> that a region of nuclear deformation should exist among the neutron-deficient nuclei in the vicinity of  $Z > 50, N < 82$ . There is additional evidence<sup>4,5</sup> that nuclei with oblate shapes exist in this region. The theoretical and experimental results agree to within 4.5% over the energy range 3.0-15.0 MeV for nuclei of Sb, Te, <sup>127</sup>I, <sup>133</sup>Cs, and Ba. We consider any evidence, in the cross sections, of oblate deformation in these nuclei to be marginal. The theoretical and experimental results for <sup>139</sup>La, Ce, <sup>141</sup>Pr, and Nd again tend to agree to within 1-3%, which is consistent with their description as spherical nuclei.

The ground-state rotational bands of certain

even-even nuclei provide some of the clearest examples of the rotational structure ( $K=0$ ) of nuclei, for example,  $^8\text{Be}$ ,  $^{24}\text{Mg}$ ,  $^{166}\text{Er}$ , and  $^{238}\text{U}$ . However, many odd- $A$  nuclei also exhibit rotational band structure and with a higher density of levels. The nuclei of  $^{147}\text{Pm}$ ,  $\text{Sm}$ ,  $\text{Eu}$ ,  $\text{Gd}$ ,  $^{159}\text{Tb}$ ,  $\text{Dy}$ ,  $^{165}\text{Ho}$ ,  $\text{Er}$ ,  $^{169}\text{Tm}$ ,  $\text{Yb}$ ,  $^{175}\text{Lu}$ ,  $\text{Hf}$ ,  $^{181}\text{Ta}$ ,  $\text{W}$ ,  $^{182}\text{W}$ ,  $^{186}\text{W}$ , and  $\text{Re}$  either lie on the edge of, or in, the heavily deformed region  $152 \leq A \leq 186$ . The average of the deviations of our data from the theoretical results over the energy range 6-13 MeV starts at about 5% for  $^{147}\text{Pm}$ , rises to 17% for  $^{169}\text{Tm}$ , and decreases again to 3-4% for  $\text{Re}$ . The behavior of the deviations is similar to the deformation in this region; namely, it increases rather rapidly to a maximum at  $^{169}\text{Tm}$  and decreases slowly over the rest of the region. We illustrate the behavior of  $^{159}\text{Tb}$ ,  $^{165}\text{Ho}$ ,  $^{169}\text{Tm}$ , and  $^{175}\text{Lu}$  in Fig. 1. Incidentally, our measurement for  $^{165}\text{Ho}$  agrees to within 1% with the only other known extensive measurement of  $\sigma_T$  for a heavily deformed rare-earth nucleus, namely, the measurements of Marshak et al.<sup>6</sup>

As one traverses the spherical region corresponding to  $\text{Os}$ ,  $\text{Ir}$ ,  $\text{Pt}$ ,  $^{197}\text{Au}$ ,  $\text{Hg}$ ,  $\text{Tl}$ ,  $\text{Pb}$ ,  $^{206}\text{Pb}$ ,  $^{209}\text{Bi}$ , the greatest deviations between the experimental and theoretical results are 4% and the average deviations are of the order of 2% or less. The change in the deviations that occurs in the transition from the rare-earth region to this spherical region is consistent with the magnitude of the deformation in the two regions. Typical examples,  $\text{Ir}$  and  $^{197}\text{Au}$ , are shown in Fig. 1.

The five actinide nuclei,  $^{232}\text{Th}$ ,  $^{233}\text{U}$ ,  $^{235}\text{U}$ ,  $^{238}\text{U}$ , and  $^{239}\text{Pu}$ , are additional examples of highly deformed nuclei. The average deviations of the experimental and theoretical results are again dramatic, with average deviations of 10% and maximum deviations of 17% over the higher and lower energy ranges. Typical examples,  $^{232}\text{Th}$  and  $^{235}\text{U}$ , are illustrated in Fig. 1. The behavior of the deviations is again consistent with the deformation in the region  $228 \leq A \leq 240$ .

We summarize the results as follows: The experimental and theoretical results agree to within 0.5-4.0% for (1) 39 spherical nuclei within  $45 \leq A \leq 144$  and (2) nine spherical nuclei within  $190 \leq A \leq 209$ . However, the experimental results deviate from the theoretical results by as much as 17% for (1) 15 deformed nuclei within  $152 \leq A \leq 186$  and (2) five deformed nuclei within  $228 \leq A$

$\leq 240$ .

It is clear from these observations that an analysis which uses the phenomenological, spherical, nonlocal optical potential of Perey and Buck adequately describes the behavior of the total cross section for fast neutrons incident upon spherical nuclei. However, it is equally clear that such an analysis yields considerably less accurate results for highly deformed nuclei. Presumably, if one could eliminate the effects of deformation upon the optical potential, then the analysis would also be adequate for these nuclei.

It is known that the effects of nuclear deformation upon the phenomenological nonlocal optical potential can artificially be eliminated by explicitly treating the strong coupling between the ground and excited states in a coupled-channel analysis.<sup>7-9</sup> We conjecture that when this contribution has been removed, the remaining effective nonlocal potential should adequately describe the total probability for the interaction of fast neutrons with any of the nuclei within  $45 \leq A \leq 240$  regardless of whether they are spherical or highly deformed. We hope to report results of a coupled-channel calculation in a future publication.

The authors would like to thank Dr. R. E. Schenter, Dr. C. W. Lindenmeier, Dr. B. R. Leonard, Jr., and Dr. R. L. Cassola for many helpful discussions.

\*Paper based on work performed under U. S. Atomic Energy Commission Contract No. AT(45-1)-1830.

<sup>1</sup>D. G. Foster, Jr., and D. W. Glasgow, Nucl. Instr. Methods **36**, 1 (1965).

<sup>2</sup>F. Perey and B. Buck, Nucl. Phys. **32**, 353 (1962).

<sup>3</sup>R. K. Sheline, T. Sikkeland, and R. Chanda, Phys. Rev. Letters **7**, 446 (1961); E. Marshalek, L. W. Person, and R. K. Sheline, Rev. Mod. Phys. **35**, 108 (1963).

<sup>4</sup>K. Kumar and M. Baranger, Phys. Rev. Letters **12**, 73 (1964).

<sup>5</sup>F. Ackermann, E. W. Otten, G. zu Putlitz, A. Schenck, and S. Ullrich, Phys. Letters **26B**, 367 (1968).

<sup>6</sup>H. Marshak, A. Langsford, C. Y. Wong, and T. Tamura, Phys. Rev. Letters **20**, 554 (1968).

<sup>7</sup>B. Buck and F. Perey, Phys. Rev. Letters **8**, 444 (1962).

<sup>8</sup>T. Tamura, Rev. Mod. Phys. **37**, 679 (1965).

<sup>9</sup>N. K. Glendenning, in Proceedings of the International School of Physics "Enrico Fermi," Course XL, edited by J. Steinberger (Academic Press, New York, 1968).